Thermo-Calc Software

TCS Al-based Alloy Database (TCAL)

Examples Collection

Document created 11/30/2020

Contents

About the Database Examples

There are examples available to demonstrate both the *validity* of the database itself as well as to demonstrate some of its *calculation* capabilities when combined with Thermo-Calc software and its Add-on Modules and features.

For each database, the type and number of available examples varies. In some cases an example can belong to both a validation and calculation type.

- *Validation* examples generally include experimental data in the plot or diagram to show how close to the predicted data sets the Thermo-Calc calculations are usually using the most recent version of the software and relevant database(s) unless otherwise specified.
- *Calculation* examples are intended to demonstrate a use case such as how the database and relevant software features would be applied to a heat treatment application, process metallurgy, soldering process, and so forth. In the case of heat treatment, it might include the result of calculating solidification segregation, determining homogenization temperature and then predicting the time needed to homogenize. There are many other examples specifically related to each database.

If you are interested in sharing your own examples using Thermo-Calc products in unique or surprising ways, or if you want to share your results from a peer reviewed paper, send an email to info@thermocalc.com.

TCS Al-based Alloy Database (TCAL) Resources

Information about the database is available on our website and in the Thermo-Calc software online Help.

- **Website**: On our website the information is both searchable and the database specific PDFs are available to download.
- **Online Help**: Technical database information is included with the Thermo-Calc software online Help. When in Thermo-Calc, press F1 to search for the same information as is contained in the PDF documents described. Depending on the database, there are additional examples available on the website.

Database Specific Documentation

- The *TCAL: TCS Al-based Alloy Database Technical Information* PDF document contains version specific information such as the binary, ternary and higher-order assessed systems, phases and models. It also includes details about the properties data (e.g. viscosity, surface tension, etc.), a list of the included elements, and summaries of the database revision history by version.
- The *TCAL: TCS Al-based Alloy Database Examples Collection* PDF document contains a series of validation examples using experimental data, and a set of calculation examples showing some of the ways the database can be used.

Go to the Aluminum-based Alloys Databases page on our website where you can access the technical information and learn more about the compatible kinetic database. Also explore further applications of Thermo-Calc to aluminum including links to resources such as publications, webinars, videos, and more.

Learn more on our website about the CALPHAD Method and how it is applied to the Thermo-Calc databases.

TCAL Validation Examples

Some diagrams are calculated with earlier versions of the database. Negligible differences might be observed if these are recalculated with the most recent version. The diagrams are updated when there are considerable or significant improvements.

In this section:

Solidification: Phase Formation

A conventional Scheil simulation provides an upper boundary for how far a solidification can deviate from equilibrium, therefore a real solidification is expected to occur between the equilibrium simulation and the Scheil simulation. In Thermo-Calc performing a Scheil simulation always triggers an equilibrium simulation. This example uses the TCS Al-based Alloy Database (TCAL).

Read more about Scheil Solidification Simulations on our website. If you are in Thermo-Calc, press F1 to search the help to learn about using Scheil.

A206 Alloy

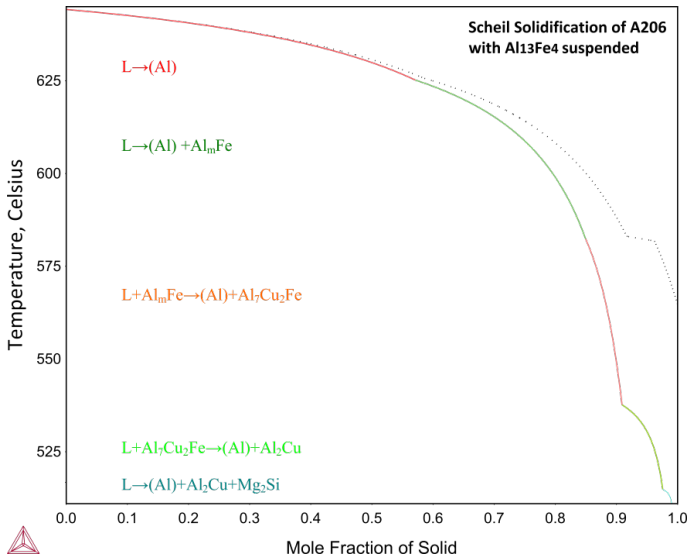

Figure 1: Scheil solidification of an A206 alloy (Al-4.58Cu-0.28Mg-0.51Fe-0.07Si-0.003Mn, wt.%) with the $Al_{13}Fe_4$ phase suspended [2014b, Chen]. According Liu et al. [2012], the metastable Al_mFe phase formed after (Al) during the solidification. The phase formation sequence and phase transformation temperatures can be well accounted for with this calculation.

Alloy AA7075

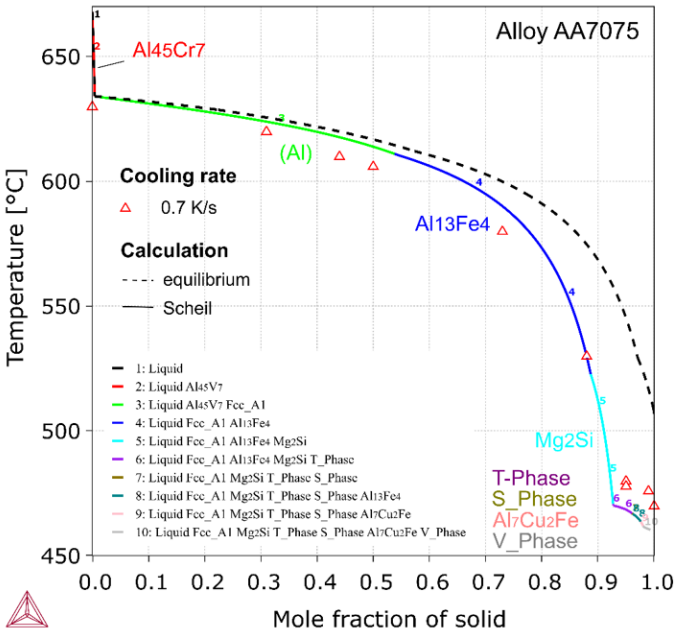

Figure 2: Equilibrium solidification and Scheil solidification simulations of alloy AA7075, compared with experimental results [1990, Backerud]. (Al), $Al_{13}Fe_4$, Mg_2Si, T-Phase and V-Phase ($MgZn_2$) are found in the microstructure as predicted from the calculation. $Al_{45}Cr_7$ forms primarily as a Cr-bearing phase, which may have been overlooked in experimental investigation due to its small amount. S-Phase was shown at the late stage of the Scheil solidification and its amount is small. Al_2Cu was experimentally observed but not shown in the calculation.

Foundry Alloy 204.2

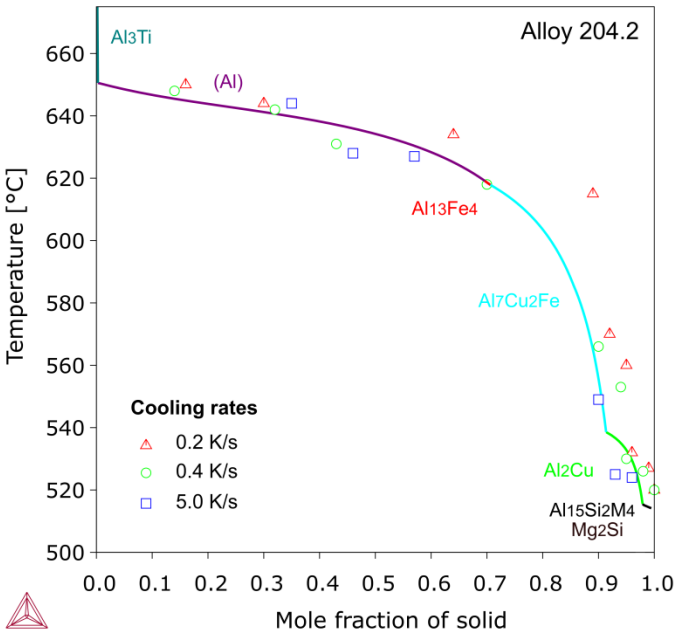

Figure 3: Scheil solidification simulation of foundry alloy 204.2 (Al-$Si_{0.08}Fe_{0.20}Cu_{4.40}Mn_{0.02}Mg_{0.22}Ti_{0.22}$, wt.%), compared with DTA experimental results [1990, Backerud]. The formation of (Al), $Al_{13}Fe_4$, Al_6Mn (Cu,Fe), Al_7Cu_2Fe and Al_2Cu was reproduced in the Scheil simulation. Al_3Ti appeared as the primary phase due to the Ti addition.

References

[1990, Backerud] L. Backerud, G. Chai, J. Tamminen, Solidification Characteristics of Aluminum Alloys in Foundry Alloys, Volume 1 and 2 (American Foundrymen's Society, Inc., 1990), p. 266.

[2012, Liu] K. Liu, X. Cao, X. G. Chen, A New Iron-Rich Intermetallic-Al m Fe Phase in Al-4.6Cu-0.5Fe Cast Alloy. Metall. Mater. Trans. A. 43, 1097–1101 (2012).

[2014b, Chen] H.-L. Chen, "Thermodynamic modeling of metastable precipitate phases in Al-Cu, Al-Fe, Al-Mg-Si, and Al-Mg-Zn based alloys" (Stockholm, Sweden, 2014), unpublished work.

Solidification: Hot Tearing Susceptibility

It is found that hot tearing susceptibility of aluminum alloys can be reasonably predicted via evaluating the terminal freezing range (TFR). In general, the wider the TFR is, the more the alloy is susceptible to hot tearing. This example uses the TCS Al-based Alloy Database (TCAL).

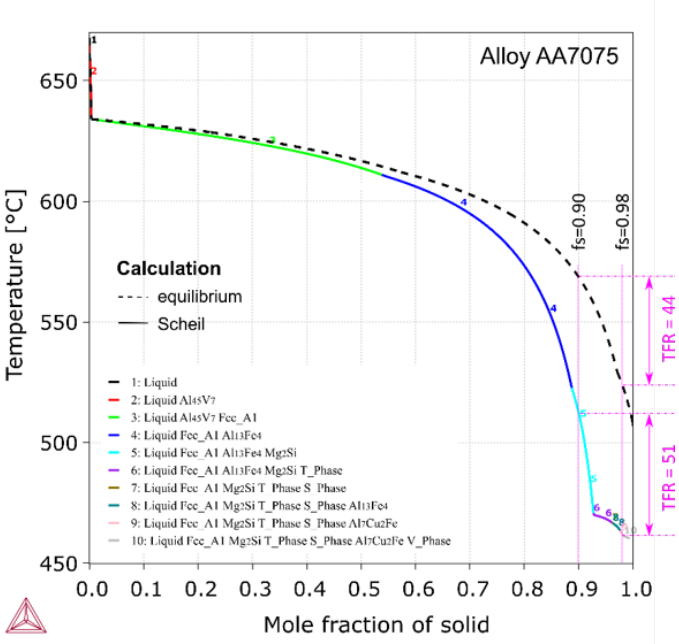

Figure 4: AA7075 alloy has a large TFR (44-51) and is prone to hot tearing.

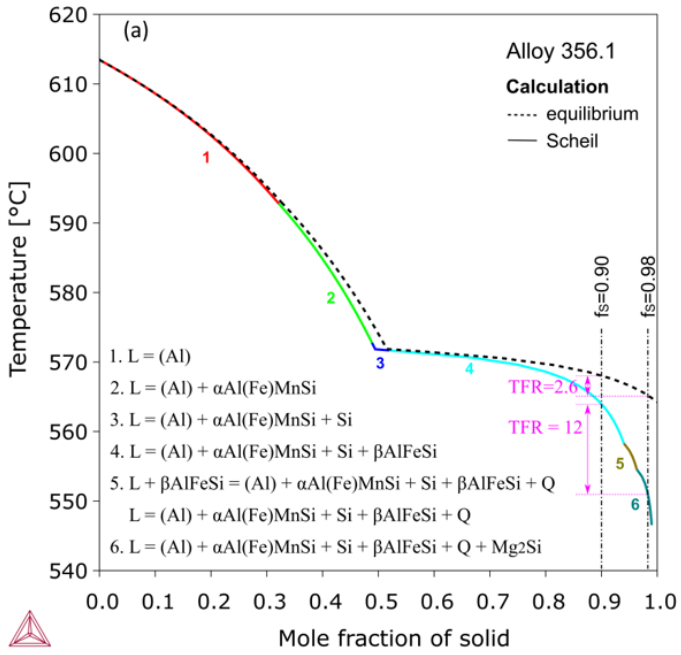

Figure 5: A356.1 alloy has a much lower TFR (2.6-12) and is much less susceptible to hot tearing. Equilibrium calculation shows an even lower value of TFR (2.6) than the Scheil simulation. This may indicate that the risk of hot tearing may be reduced by changing experimental conditions, e.g. lowering the cooling rate or using preheated casting molds.

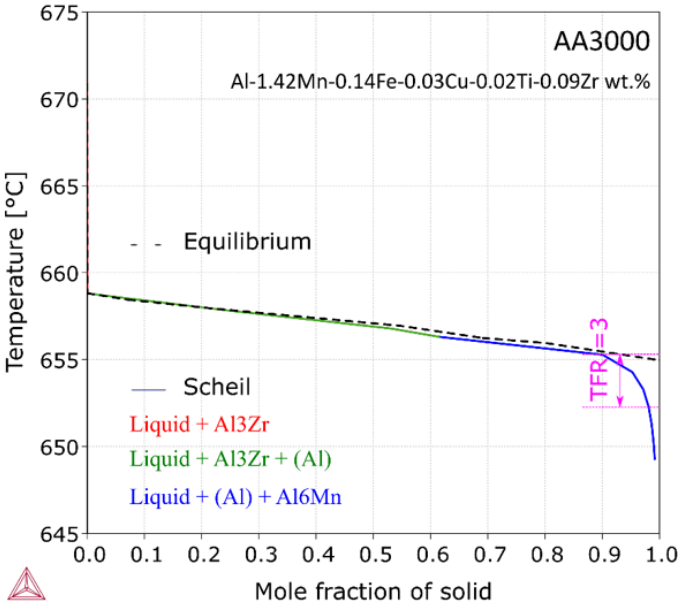

Figure 6: AA3000 alloy has an even lower TFR and has been reported to be insusceptible to hot tearing.

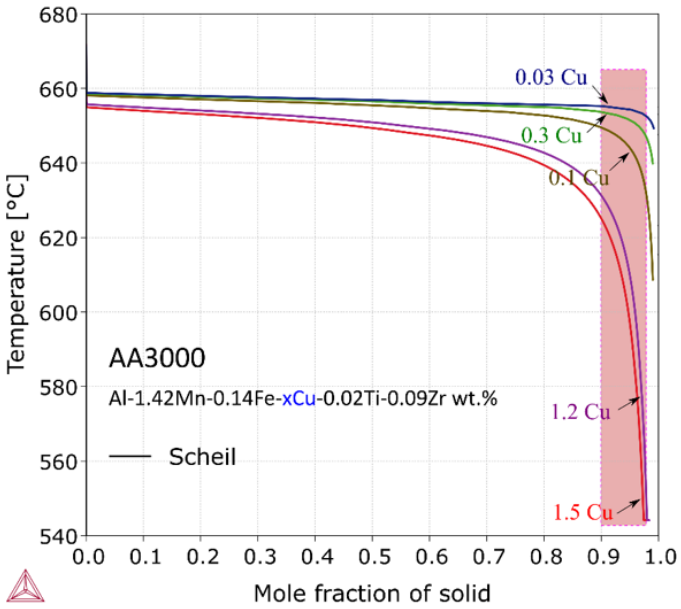

Figure 7: Adding Cu to AA3000 alloy significantly increases the susceptibility and worsens the castability.

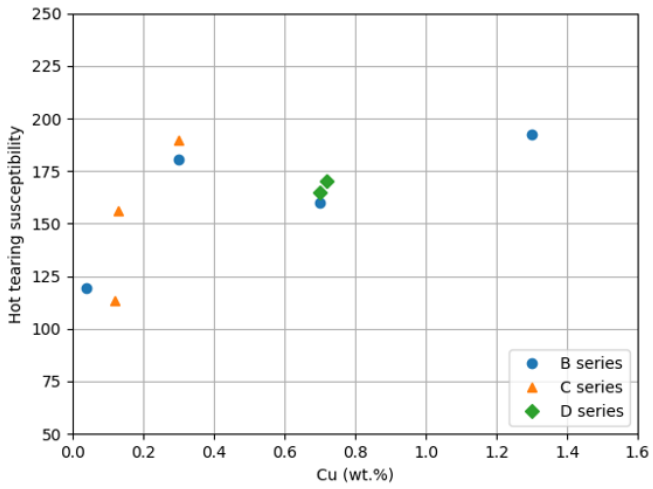

Figure 8: The recent experimental investigations by Razaz [2019] reported that "a similar increase in HTS with Cu additions from 0.3 to 1.2 wt.% was proven" in 3000 alloys. The data are somewhat scattered because there are three groups of alloys and the contents of the other alloying elements are not exactly the same even for each group, but one can evidently see the trend that HTS increases with Cu additions.

Reference

[2019, Razaz] G. Razaz, T. Carlberg, Hot Tearing Susceptibility of AA3000 Aluminum Alloy Containing Cu, Ti, and Zr, Metall. Mater. Trans. A Phys. Metall. Mater. Sci., (2019).

Solidification: Back Diffusion

Further to the simulation shown in Solidification: Hot Tearing Susceptibility of an AA7075 alloy (0.2 Si, 0.25 Fe, 1.6 Cu, 0.15 Mn, 2.5 Mg, 5.6 Zn, wt.%), this example, also using the TCS Al-based Alloy Database (TCAL), considers back diffusion. The data are from Backrud [1990] and correspond to a cooling rate of 0.7 K/s. As expected, the simulated curve at 0.7 K/s lies between the equilibrium curve and the Scheil curve and agrees much better with the experimental data. By comparison, an additional simulation at 100 K/s is run and the resulting curve is close to the Scheil one.

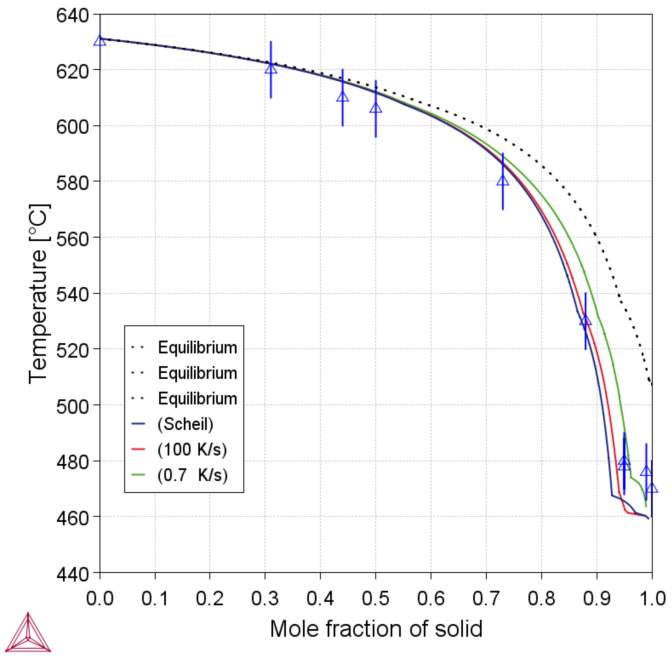

Figure 9: Solidification simulations of the AA7075 alloy (0.2 Si, 0.25 Fe, 1.6 Cu, 0.15 Mn, 2.5 Mg, 5.6 Zn, wt.%) with the conventional Scheil model or taking into account back diffusion at different cooling rates. The dashed line corresponds to equilibrium calculation.

Reference

[1990, Backrud] L. Backerud, G. Chai, J. Tamminen, Solidification Characteristics of Aluminum Alloys in Foundry Alloys, Volume 1 and 2 (American Foundrymen's Society, Inc., 1990), p. 266.

Solidification: Microsegregation

Microsegregation can be easily predicted by the formation of grain boundaries phases and the composition profile of the (Al) matrix phase. The former has been demonstrated in another example, Solidification: Phase Formation. Figure 10 shows the (Al) profiles in Al-2, 4, and 8 wt.% Cu alloys from Scheil simulations using the TCS Al-based Alloy Database (TCAL). In the Figure 11 micrograph, the simulated profiles indicate that:

- The cores of (Al) grains are lean in Cu. Increasing the alloy composition increases the Cu content in the cores.
- The maximum Cu content in the outer rims of (Al) grains is independent of the alloy composition.
- The outer rims are thickened with increasing the Cu content in the alloys.

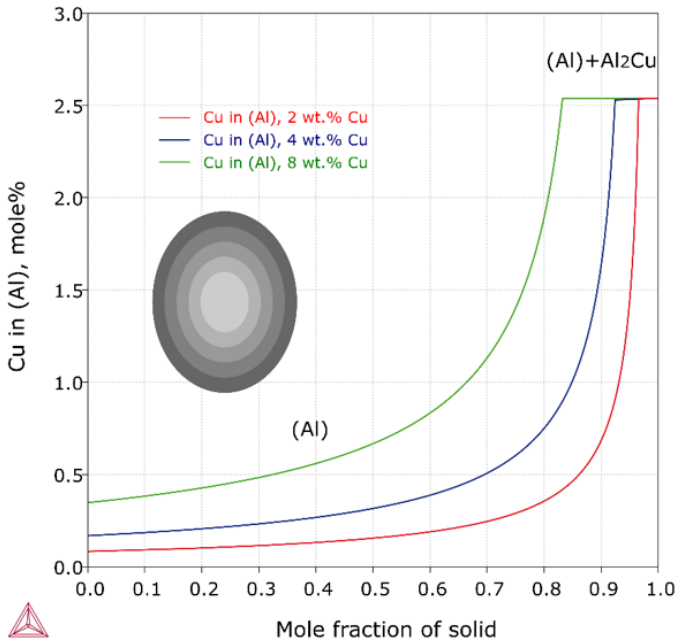

Figure 10: The (Al) profiles in Al-2, 4, and 8 wt.% Cu alloys from Scheil simulations.

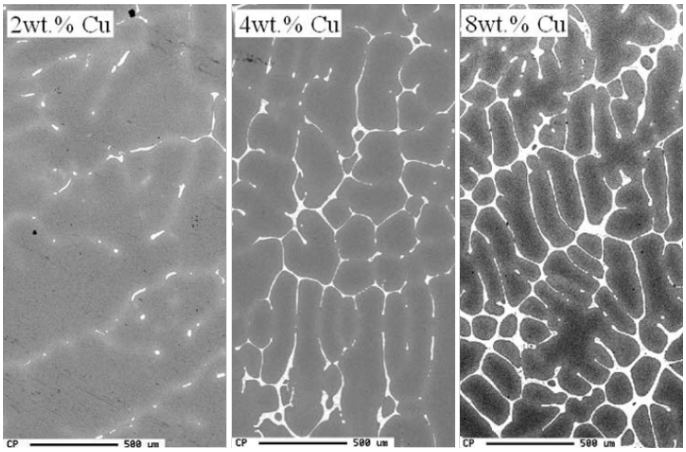

Figure 11: A micrograph from Kurum [2005]. Details described in the text.

Reference

[2005, Kurum] E. C. Kurum, H. B. Dong, J. D. Hunt, Microsegregation in Al-Cu Alloys. Metall. Mater. Trans. A, 36, 3103 (2005).

Homogenization / Solution Treatments: Al-Si Alloys

In some cases, the heating temperature can only be preliminarily determined with a stepping calculation. It should be optimized, together with the heating time, based on the Diffusion Module (DICTRA) simulations.

This example, using the TCS Al-based Alloy Database (TCAL), shows simulated dissolution of Si particles at 500 °C, 530 °C, and 560 °C with a multiple-cell approach (Figure 12). 500 °C is too low since the particles cannot be fully dissolved even after three (3) hours. By comparison, the particles disappear within 15 minutes at 560 °C and one (1) hour at 530 °C. You can choose either temperature or a temperature between taking into account other factors, such as energy consumptions, risks of melting, etc.

Read more about the Diffusion Module (DICTRA) on our website. If you are in Thermo-Calc, press F1 to search the help to learn about the available settings included with the Add-on Module.

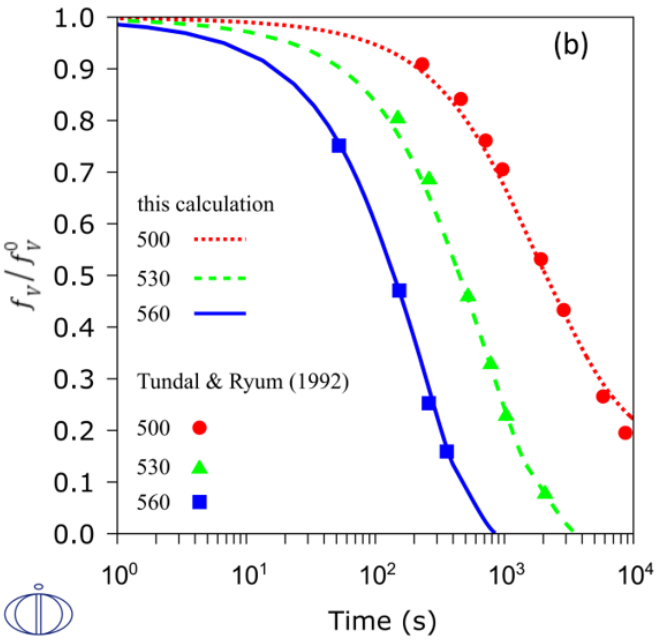

Figure 12: Simulated dissolution of Si particles at 500 °C, 530 °C, and 560 °C for multiple-cell approaches.

Homogenization / Solution / Aging Treatments: AA7093

Solution treatment is to dissolve (fully or partly) particles that form at the grain boundaries into the (Al) matrix. *Homogenization* is to eliminate or reduce the composition segregation in the (Al) matrix. Very often these kinds of treatments can be performed at the same time and thus are not distinguished. Temperature and time are the most important parameters that need to be optimized for a heat treatment. This example uses the TCS Al-based Alloy Database (TCAL).

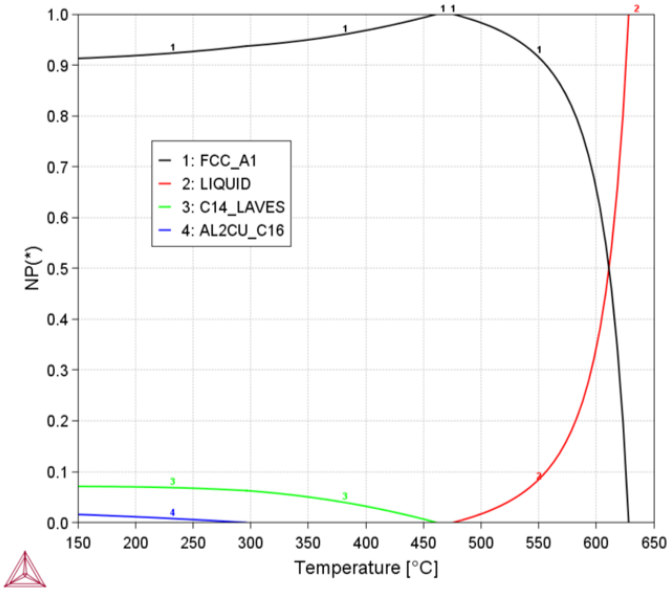

Figure 13: Solution treatment showing a narrow window of 462-475 °C of single (Al) phase which was predicted for alloy AA7093 (Al-10.3Zn-1.6Cu-2Mg, wt. %).

For a solution treatment, the heating temperature can be preliminarily determined according to an equilibrium stepping. A narrow window of 462-475 °C of single (Al) phase was predicted for alloy AA7093: Al-10.3Zn-1.6Cu-2Mg, wt. %. In such cases, the temperature may be determined as the mean value independently of the heating time. This agrees well with the experimental temperature of 470 °C by Marlaud [2010].

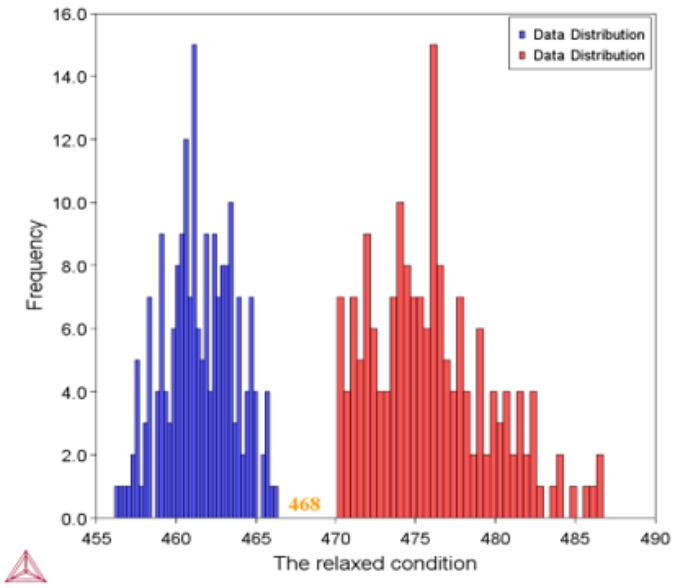

Figure 14: Alloy AA7093 uncertainty calculations using the Property Model Calculator. Temperatures are calculated at 200 compositions and the frequency of each obtained temperature is plotted.

Since the composition of the AA7093 alloy may vary within the specification tolerance (i.e. Zn 10.3±0.5, Cu 1.6±0.1, Mg 2.0±0.1), it is useful to investigate how the composition uncertainty affects the temperature range corresponding to the single-(Al)-phase region. With the Property Model Calculator in Thermo-Calc Graphical Mode you can easily take into account such an uncertainty in calculations. In Figure 14, the temperatures are calculated at 200 compositions and the frequency of each obtained temperature is plotted. A single (Al) phase can still be attained for all the possible compositions, while the window is further narrowed down. The present evaluation suggests that 468 °C is the optimal heating temperature.

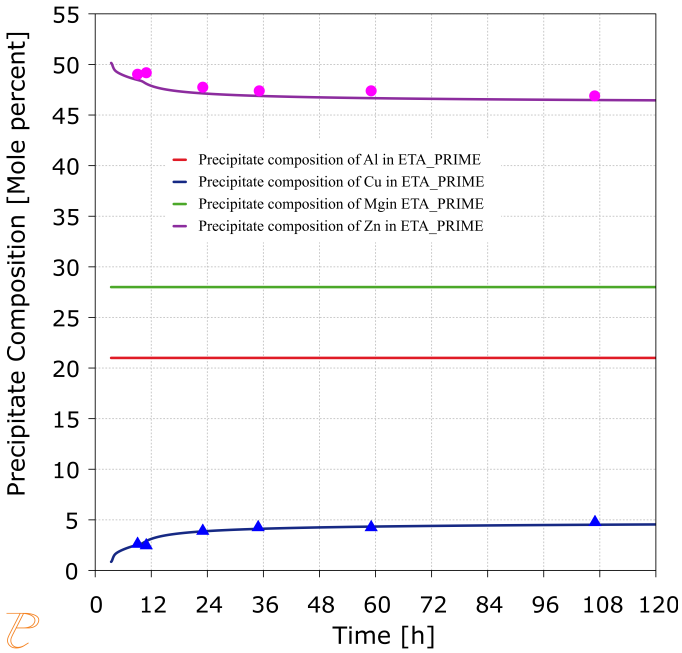

Figure 15: A simulation of the precipitation during the aging treatment showing the contents of the solutes in the η' precipitates for the 7093 alloy. Curves are from the Precipitation Module (TC-PRISMA) simulations and symbols are experimental data

η' is a major strengthening precipitate in the 7000 series of alloys. After being quenched from the homogenization, the 7093 alloy was aged (heating procedure: from 20 °C to 120 °C at 30 °C/h, 30 °C for 6 h, from 120 °C to 135 °C at 15 °C/h, and 135 °C) by Marlaud [2010]. Figure 15 is an example simulating the precipitation during the aging treatment with the contents of the solutes in the η' precipitates.

Read more about the Precipitation Module (TC-PRISMA) on our website. If you are in Thermo-Calc, press F1 to search the help to learn about the available settings included with the Add-on Module.

Reference

[2010, Marlaud] T. Marlaud, A. Deschamps, F. Bley, W. Lefebvre, B. Baroux, "Influence of alloy composition and heat treatment on precipitate composition in Al-Zn-Mg-Cu alloys", Acta Mater. 58 (2010) 248-260.

Homogenization / Solution /Aging Treatment: 6005

According to this equilibrium calculation using the TCS Al-based Alloy Database (TCAL), it is impossible to attain a single (Al) phase for AA6005 alloy (Al-0.82Si-0.55Mg-0.016Cu-0.5Mn-0.2Fe, wt. %) after a solution treatment.

The temperature of 530 °C was chosen considering these factors:

- it is sufficient high to fully dissolve the Mg_2Si compound so as to maximize the amount of precipitates during aging,
- the Al15Si2M4 phase can be dissolved to a large extent, and
- it leaves a margin to the incipient melting.

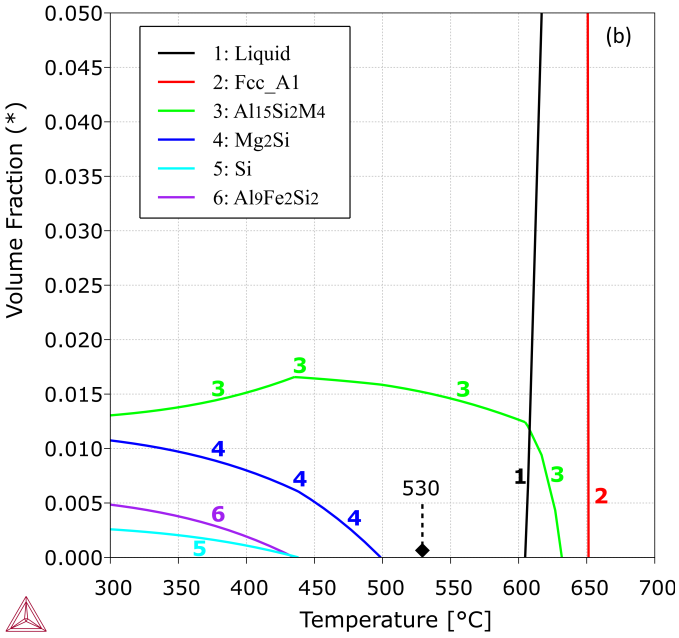

Figure 16: Equilibrium calculation for AA6005 alloy (Al-0.82Si-0.55Mg-0.016Cu-0.5Mn-0.2Fe, wt. %) after a solution treatment. See the text for discussion.

The following example is to simulate the precipitation of β'' in the (Al) matrix in the 6005 alloy. The composition of the (Al) solution, 0.562 wt.% Mg, 0.016 wt.% Cu, 0.607 wt.% Si, 0.054 wt.% Mn and 0.002 wt.% Fe, was calculated first at the solution treating temperature of 530 °C and it is slightly different from the nominal alloy composition. The figure below shows simulated mean radius and aspect ratio of β'' precipitates at 185 °C.

Read more about the Precipitation Module (TC-PRISMA) on our website. If you are in Thermo-Calc, press F1 to search the help to learn about the available settings included with the Add-on Module.

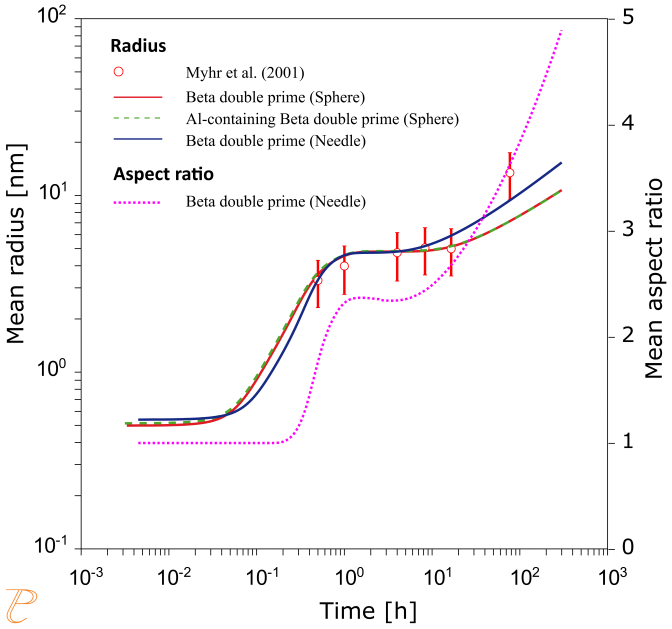

Figure 17: Simulated mean radius and aspect ratio of β'' precipitates at 185 °C. This plot uses the add-on Precipitation Module (TC-PRISMA).

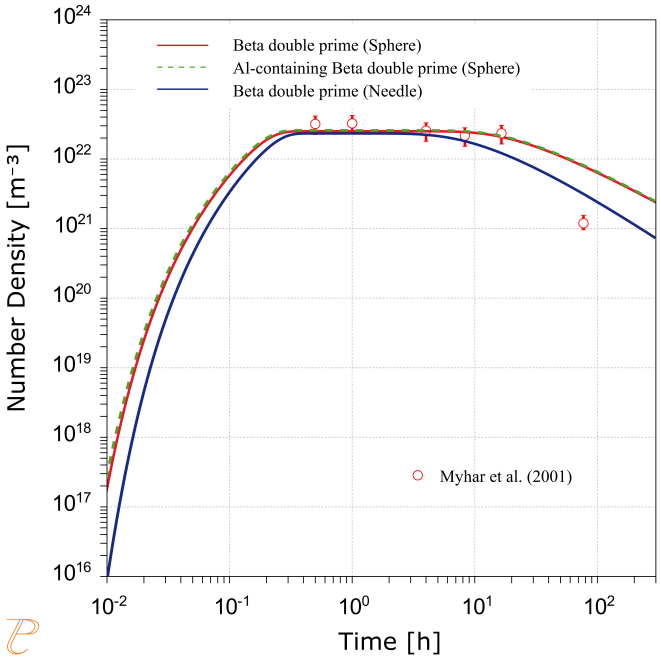

Figure 18: Simulated number density of β'' precipitates in AA6005 alloy at 185 °C. This plot uses the add-on Precipitation Module (TC-PRISMA).

Electrical Resistivity and Thermal Conductivity

Using Thermo-Calc and with the TCS Al-based Alloy Database (TCAL), you can calculate the quantities of a phase ϕ with the variables ELRS(ϕ) and THCD(ϕ), or a system (i.e. alloy) with ELRS and THCD. You can also calculate the derived quantities, i.e. electrical conductivity (ELCD), thermal resistivity (THRS) and thermal diffusivity (THDF) in a similar way.

The TCS Al-based Alloy Database includes electrical resistivity (ELRS) and thermal conductivity (THCD) starting with version 7 (TCAL7).

You can find information on our website about the thermophysical properties that can be calculated with Thermo-Calc and the Add-on Modules. Additional resources will also be made available on our website in the near future so keep checking back or subscribe to our newsletter.

Wrought Al Alloys

Figure 19 compares the calculated ELRS with tabulated data for 35 wrought Al alloys after “O” heat treatments. For each alloy, an equilibrium calculation is first performed at 350 °C (assumed annealing temperature), so phases that are present, and their fractions and compositions are obtained with Thermo-Calc. Then the temperature is changed to 25 °C (measuring temperature), and the value of ELRS is directly retrieved without equilibrium-computing.

For alloys produced with other treatment, sometimes you have to take into account impacts of deformations and precipitations, etc.. For as-cast alloys, you can use Scheil simulations (with or without back diffusion) to predict the phases, as well as the fractions and compositions, and then evaluate ELRS and THCD appropriately.

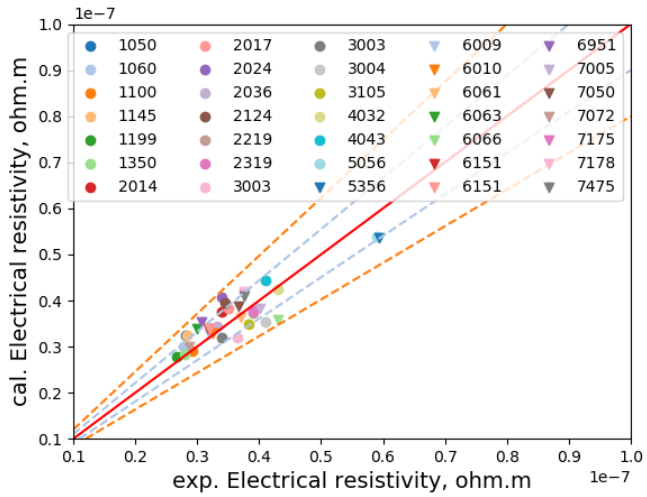

Figure 19: Compares the calculated ELRS with tabulated data for 35 wrought Al alloys after "O" heat treatments. The ELRS of an alloy is calculated as the mechanical mixing of individual phases according to volume fractions, with a calibration for interface scattering. The calibration is assumed to be proportional to the total fraction of grain boundary phases with a coefficient of +4.83e-8 ohm.m. The red solid line indicates where calculated values are equal to experimental data. The light blue dashed lines mark the limits for 10 % deviations and the orange dashed lines for 20 % deviations. The data are from NDT [2002].

Equiatomic Single FCC_A1 Alloys

The phase equilibria may not be valid beyond an Al-rich region in multicomponent alloys. The evaluation of ELRS and THCD is based on the phase constitutions from calculations and simulations with the thermodynamic database, so in principle the current database (TCAL7) of ELRS and THCD is applicable only to Al alloys as well. The following example, however, demonstrates that it can reasonably predict the ELRS and THCD for Al-free equiatomic FCC_A1 alloys. This is because these alloys were known to be of FCC_A1 single phase, so you do not have to think about the phase equilibria.

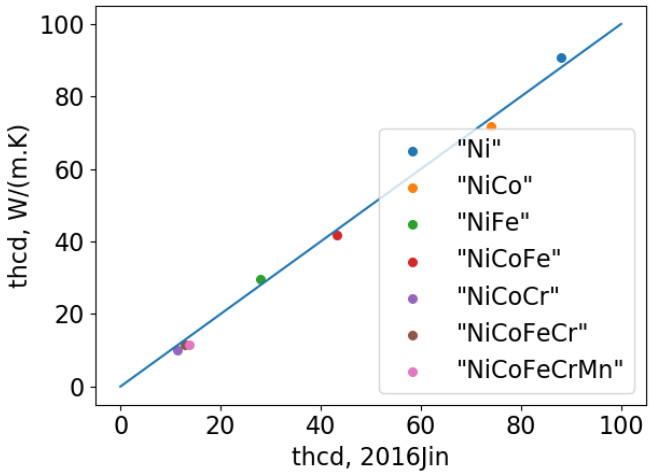

Figure 20: Calculated electrical resistivity (ELRS) of equiatomic FCC_A1 alloys. Data are from Jin [2016].

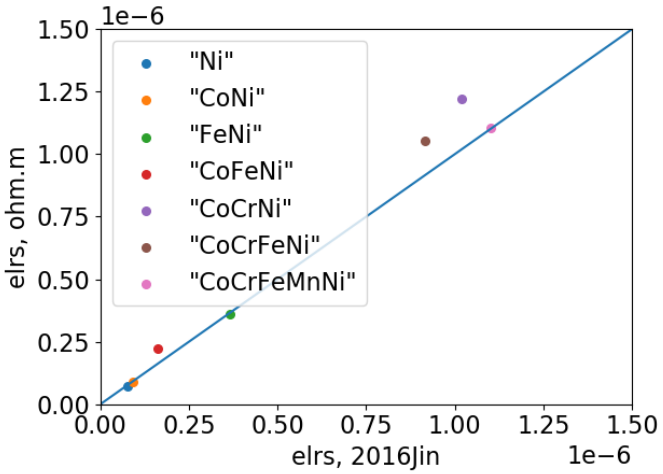

Figure 21: Calculated thermal conductivity (THCD) of equiatomic FCC_A1 alloys. Data are from Jin [2016].

Electrical Resistivity of Pure Ni

Figure 22 (left) compares the calculated electrical resistivity of pure Ni with experimental data from Chu et al. [1982]. There is a magnetic contribution to the resistivity, which is described with

$$\rho_m = \rho_{spd} \cdot \left(1 - e^{\left(-\frac{3}{2}\left(\frac{T}{T_c}\right)^3\right)}\right)$$

implemented in Thermo-Calc. Figure 22 (right) compares the calculated thermal conductivity of pure Ni with experimental data from Ho et al. [1972].

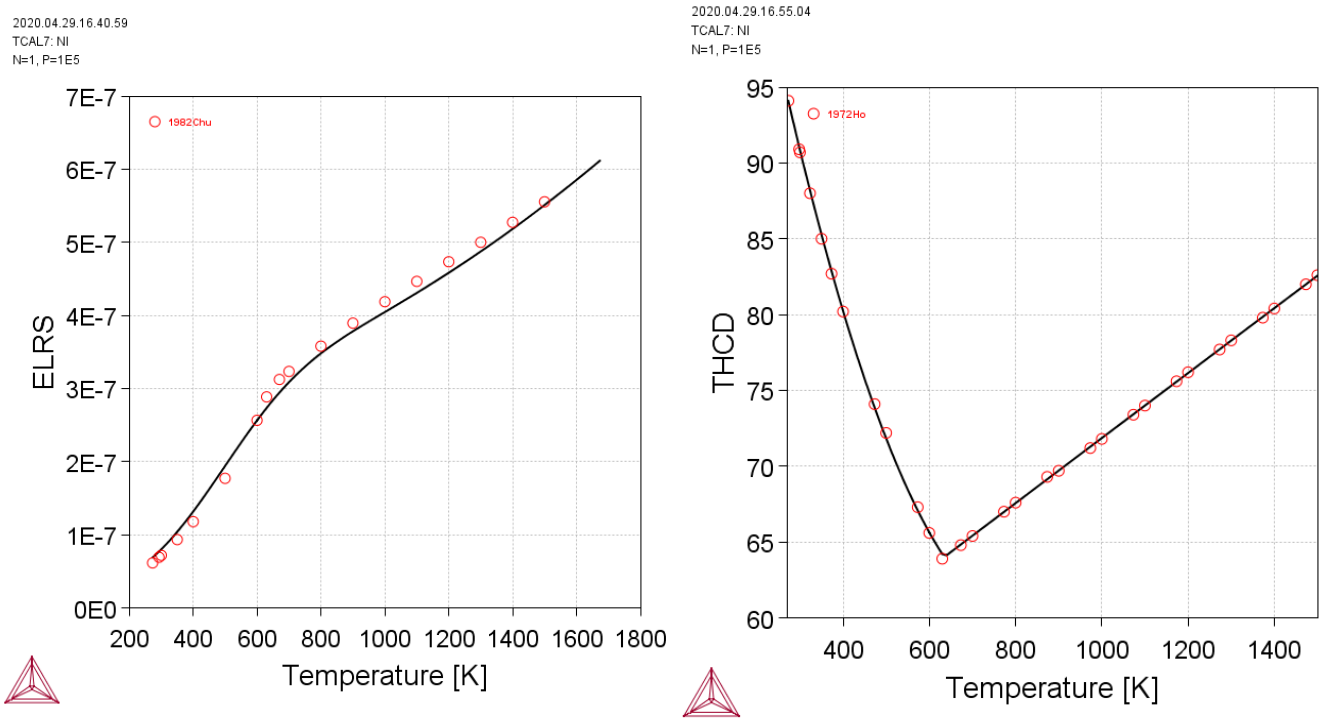

Figure 22: (left) electrical resistivity and (right) thermal conductivity of pure Ni.

Electrical Resistivity of Al-Mg

Figure 23 shows calculated electrical resistivity of the Al-Mg FCC_A1 solid solution in a wide temperature range from 250 K to 850 K, in comparison with data recommended by Ho et al. [1983], which were from "annealed" alloys. It should be noted that the calculations are performed with `global_minimization off` and with all the phases suspended except for FCC_A1. This is because the FCC_A1 single phase, which was obtained after being annealed and quenched, is assumed not to decompose or transform to another phase while it was exposed to the measuring temperatures for a short period of time.

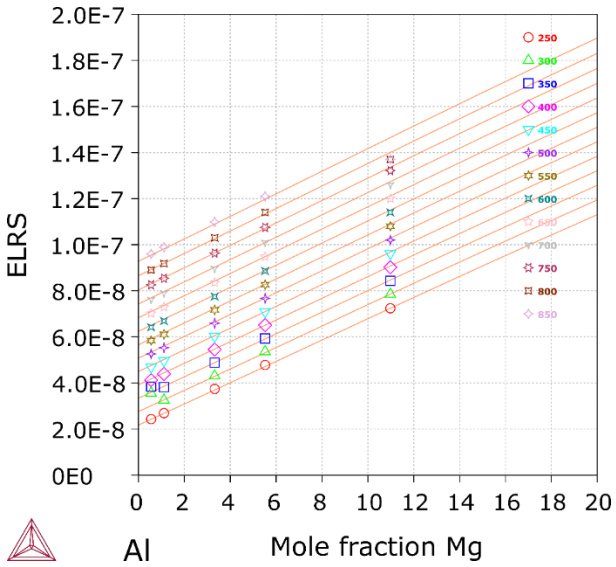

Figure 23: Electrical resistivity of Al-Mg single phase solid solution.

References

[1972, Ho] C. Y. Ho, R. W. Powell, P. E. Liley, Thermal Conductivity of the Elements. J. Phys. Chem. Ref. Data. 1, 279–421 (1972).

[1982, Chu] T. K. Chu, C. Y. Ho, “Electrical resistivity of Chromium, Cobalt, Iron, and Nickel- CINDAS Report 60” (West Lafayette, Indiana, 1982).

[1983, Ho] C. Y. Ho, M. W. Ackerman, K. Y. Wu, T. N. Havill, R. H. Bogaard, R. A. Matula, S. G. Oh, H. M. James, Electrical Resistivity of Ten Selected Binary Alloy Systems. J. Phys. Chem. Ref. Data. 12, 183–322 (1983).

[2002, NDT] Conductivity and Resistivity Values for Aluminum & Alloys, Compiled by the Collaboration for NDT Education, March 2002.

[2016, Jin] K. Jin, B. C. Sales, G. M. Stocks, G. D. Samolyuk, M. Daenen, W. J. Weber, Y. Zhang, H. Bei, Tailoring the physical properties of Ni-based single-phase equiatomic alloys by modifying the chemical complexity, Scientific Reports 6, 20159 (2016).

TCAL Calculation Examples

Some diagrams are calculated with earlier versions of the database. Negligible differences might be observed if these are recalculated with the most recent version. The diagrams are updated when there are considerable or significant improvements.

In this section:

Al-Li

Lithium (Li) is an important alloying element to some 8000 series (Al-Li based) and 2000 series (Al-Cu-Li-based) of aluminum alloys. In this example using the TCS Al-based Alloy Database (TCAL), the AL1LI2 stable phase is included in the equilibrium phase diagram (Figure 24) and the $L1_2$-type metastable precipitate Al_3Li (named as AL_3X, X=Er, Li, Sc, Ti, Zr) is modeled.

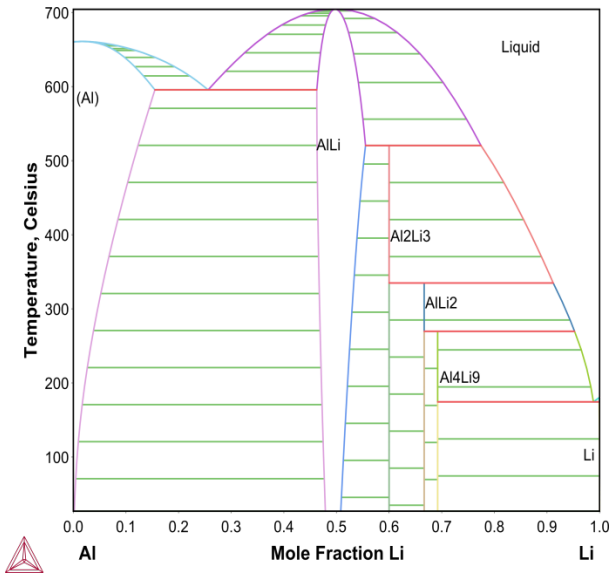

Figure 24: Calculated Al-Li phase diagram [1989, Saunders; 2012/2017b,Chen].

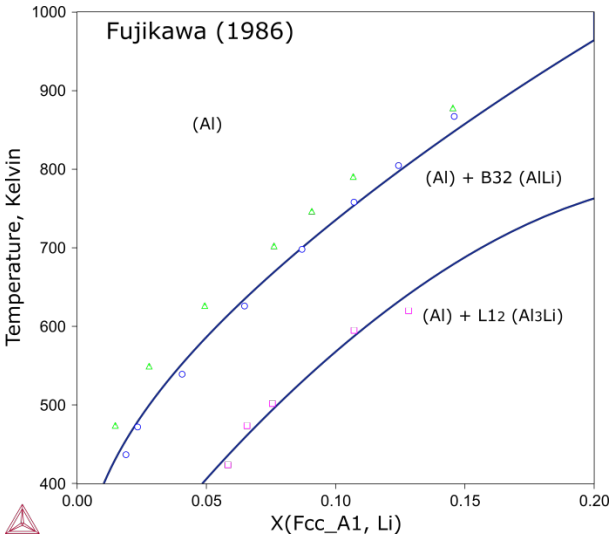

Figure 25: Calculated (Al) solvi in the Al-Li system (references from Figure 24) in comparison with the data from Fujikawa [1986].

References

[1986, Fujikawa] S. Fujikawa, Solvuses of delta' phase (Al3Li) and delta phase (AlLi) in Al-Li alloys. J. Japan Inst. Light Met. 36, 771–777 (1986).

[1989, Saunders] N. Saunders, Calculated stable and metastable phase equilibria in Al-Li-Zr alloys. Zeitschrift fur Met. 80, 894–903 (1989).

[2012/2017b,Chen] H.-L. Chen, "Modeling of the AlLi2 and Al3Li phases in the Al-Li binary system", unpublished work, 2012a/2017b.

Al-Er

As a rare earth element, Er recently attracted research interest. The Er addition forms the $L1_2$-type precipitate Al_3Er (named as AL_3X, X=Er, Li, Sc, Ti, Zr). This is a stable phase and its melting temperature is higher than that of Al. This example uses the TCS Al-based Alloy Database (TCAL).

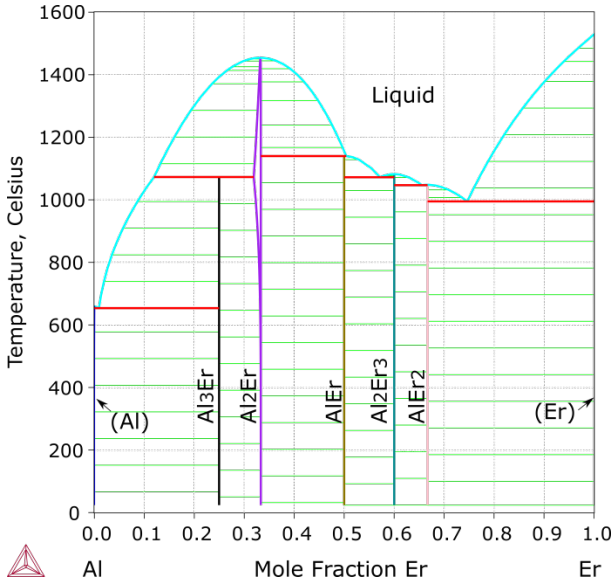

Figure 26: Calculated Al-Er phase diagram, where the Er solubility in (Al) is evaluated [Chen, 2017a].

Reference

[Chen, 2017a] H.-L. Chen, "Thermodynamic modeling of the Er-X (X = Ag, Al, Fe, Si, Zr) binary and Al-Er-X (X=Cu, Fe, Mg) ternary systems" (Stockholm, Sweden, 2017), unpublished.

Al-Fe-Si

Al-Fe-Si is a core system, as Fe and Si exist in all aluminum alloys either as a common alloying element or an inevitable impurity. The two Al-Fe-Si compounds, τ_5: α-Al_8Fe_2Si and τ_6: β-$Al_9Fe_2Si_2$, are frequently observed in aluminum alloys. Additionally, $\tau_4$may form in high-Si aluminum alloys. This example uses the TCS Al-based Alloy Database (TCAL).

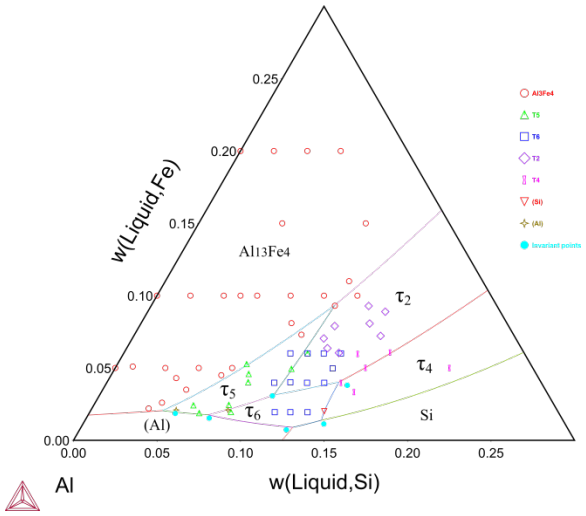

Figure 27: Calculated Al-Fe-Si liquidus projection (τ_5: α-AlFeSi; τ_6: β-AlFeSi), (a) in the Al-rich corner. The invariant points are from Pontevichi et al. [2004] and Bosselet et al. [2004]. The remaining data from Takeda and Mutuzaki [1940], Munson [1967] and Zakharov et al. [1988].

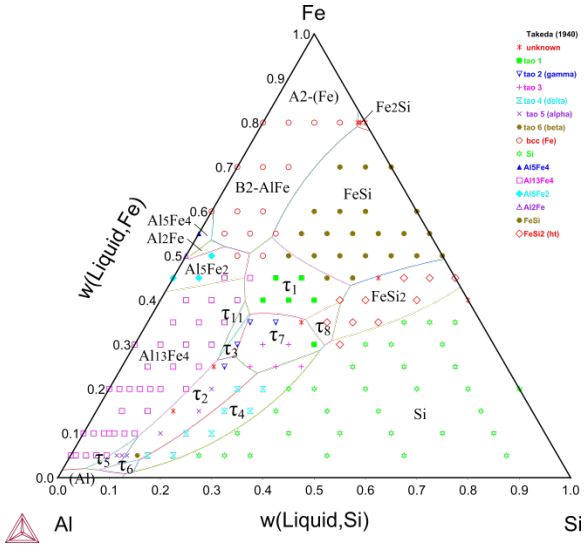

Figure 28: Continuing from Figure 27 this is over the entire compositional range, with the data from Takeda and Mutuzaki [1940].

References

[1940, Takeda] S. Takeda, K. Mutuzaki, The equilibrium diagram of the Fe–Al–Si system. Tetsu-to-Hagane. 26, 335–361 (1940).

[1967, Munson] D. Munson, A Clarification of the Phases Occurring in Aluminium-Rich Aluminium-Iron-Silicon Alloys, with Particular Reference to the Ternary Phase α-AlFeSi. J. Inst. Met. 95, 217–219 (1967).

[1988, Zakharov] A. M. Zakharov, I. T. Gulman, A. A. Arnold, Y. A. Matsenko, Phase diagram of the Aluminium-Silicon-Iron system in the concentration range of 10-14% Si and 0-3% Fe. Russ. Metall. 3, 177–180 (1988).

[2004, Bosselet] F. Bosselet, S. Pontevichi, M. Sacerdote-Peronnet, J. C. Viala, Experimental measurement of the Al-Fe-Si isothermal section at 1000 K. J. Phys. IV. 122, 41–46 (2004).

[2004, Pontevichi] S. Pontevichi, F. Bosselet, F. Barbeau, M. Peronnet, J. C. Viala, Solid-liquid phase equilibria in the Al-Fe-Si system at 727 °C. J. Phase Equilibria Diffus. 25, 528–537 (2004).

Al-Mn-Si

Al-Mn-Si is another core system to aluminum alloys. Mn is often added to suppress the formation of the detrimental τ_5: α-Al_8Fe_2Si and τ_6: β-$Al_9Fe_2Si_2$, via forming the α-AlMnSi phase (named as AL15SI2M4, M=Cr, Fe, Mn, Mo). The α-AlMnSi phase originates in the Al-Mn-Si ternary system and extends towards the Al-Fe-Si system via the substitution of Fe for Mn. The substitution of Cr and Mo for Mn is also modeled in the TCS Al-based Alloy Database (TCAL).

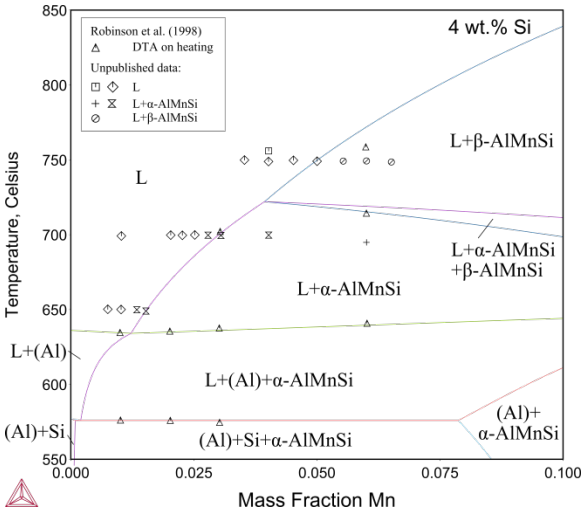

Figure 29: Al-Mn-Si vertical section at 4 wt. % Si (β-AlMnSi: τ_8; α-AlMnSi: τ_9) [2014a, Chen].

Reference

[2014a, Chen] H. Chen, Q. Chen, Y. Du, J. Bratberg, A. Engström, Update of Al-Fe-Si, Al-Mn-Si and Al-Fe-Mn-Si thermodynamic descriptions - TNMSC. Chinese J. Nonferrous Met. 24, 2041–2053 (2014).

Al-Fe-Mn-Si

Adding a small amount of Mn may promote the formation of the α-AlMnSi phase (named as AL15SI2M4, M=Cr, Fe, Mn, Mo). In fact, it competes with Al-Fe-Si compounds and forms during the casting of a wide variety of aluminum alloys. This example uses the TCS Al-based Alloy Database (TCAL).

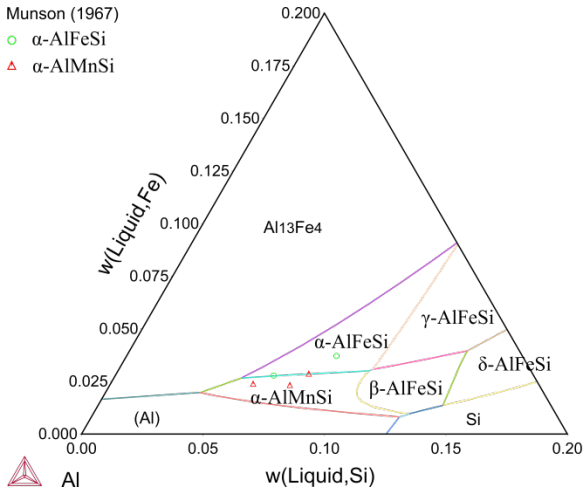

Figure 30: Al-Fe-Mn-Si liquidus surface at 0.3 wt. % Mn. (α-AlFeSi: τ_5; β-AlFeSi: τ_6; γ-AlFeSi: τ_2; δ-AlFeSi: τ_4; α-AlMnSi: τ_9) [2014a, Chen].

Reference

[2014a, Chen] H. Chen, Q. Chen, Y. Du, J. Bratberg, A. Engström, Update of Al-Fe-Si, Al-Mn-Si and Al-Fe-Mn-Si thermodynamic descriptions - TNMSC. Chinese J. Nonferrous Met. 24, 2041–2053 (2014).

Al-Cu-Mg-Zn

The Al-Cu-Mg-Zn quaternary system is the basis of the 7000 series of wrought Al alloys. The formation of the major compounds such as Al2Cu, S_PHASE, T_PHASE, V_PHASE, and M (aka. η, modeled as C14_LAVES) is essentially determined by the quaternary phase equilibria. Small additions of other alloying elements such as Fe and Mn may form additional compounds, while the formation of those major compounds is barely affected. The 7000 series are heat treatable and a typical solution treatment is performed around 460 °C. This example uses the TCS Al-based Alloy Database (TCAL).

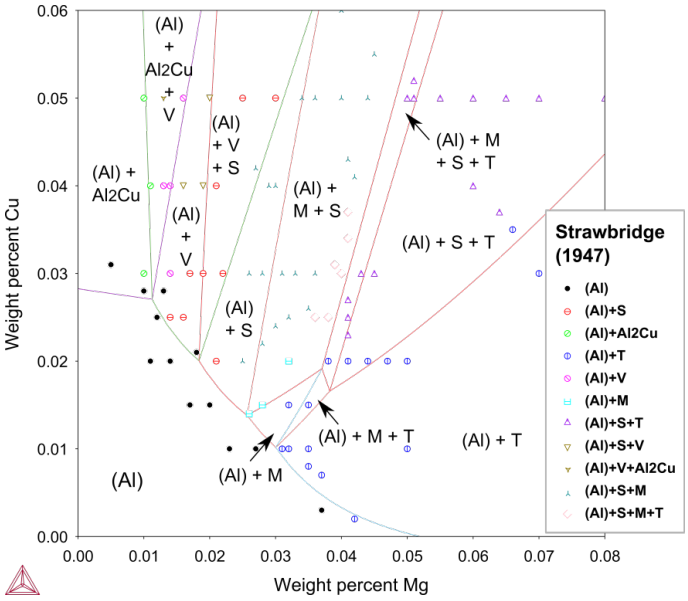

Figure 31: Calculated isothermal sections of the Al-Cu-Mg-Zn system at 460 °C: at 8 wt. % Zn [Chen, 2012b] with experimental data from Strawbridge et al. [1948].

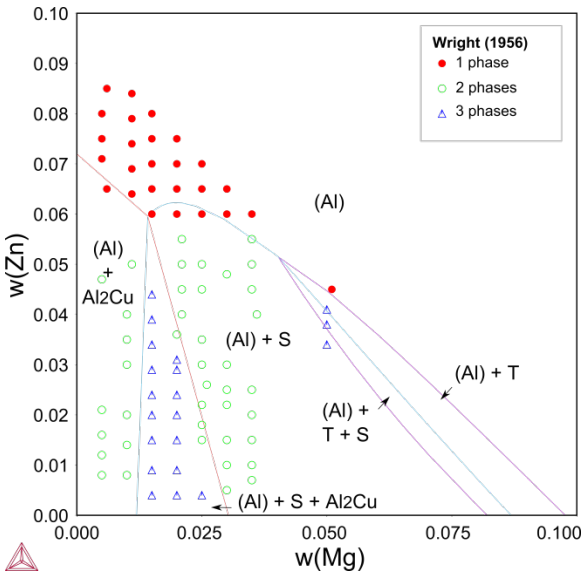

Figure 32: Calculated isothermal sections of the Al-Cu-Mg-Zn system at 90 wt.% Al with experimental data from Wright [1956].

References

[1948, Strawbridge] D. J. Strawbridge, A. Little, The Constitution of Aluminium Copper Magnesium Zinc Alloys At 460 °C. J. Inst. Met. 74, 191–225 (1948).

[1956, Wright] E. H. Wright, "Equilibrium relations at 460 °C in aluminum-copper-magnesium-zinc alloys of high purity" (Internal Report 13–56-EC2, Aluminum Research Laboratories, Aluminum Company of America, 1956).

[2012b, Chen] H.-L. Chen, "Thermodynamic assessment of the Al-Cu-Mg-Zn(-Fe) and Al-Cu-Mg-Si multicomponent alloy systems" (Stockholm, Sweden, 2012), unpublished work.

Minor Alloying Elements

Al-Cr

Many minor alloying elements and related systems are modeled in the TCS Al-based Alloy Database (TCAL). Cr is one of them. In the first place, and in order to reliably predict the formation of relevant compounds, the solubility of these elements in the melt and the (Al) solid solution must be well modeled.

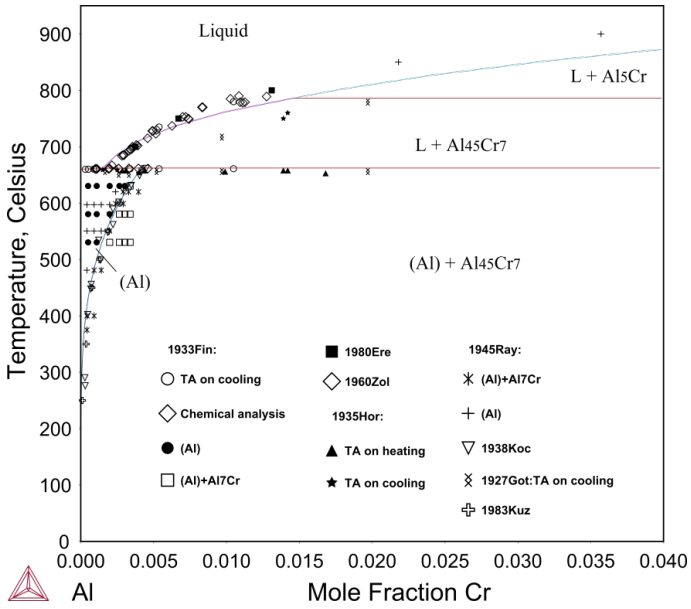

Figure 33: Calculated Al-rich Al-Cr binary phase diagram. Experimental data are from Fink and Freche [1933], Raynor and Little [1945] and Eremenko et al. [1980].

Al-Sn-Zn

Sn is an important minor alloying element in aluminum alloys. Many Sn-containing systems have been assessed since TCS Al-based Alloy Database version 5 (TCAL5).

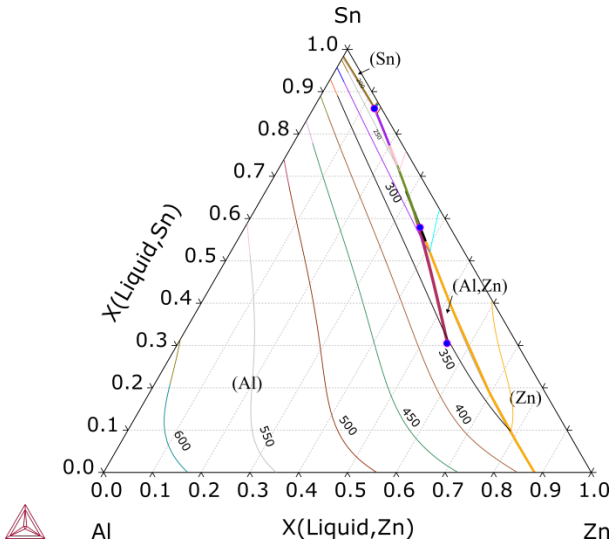

Figure 34: Al-Sn-Zn liquidus surface projection with isotherms [2017c, Chen].

References

[1933, Fink] W. L. Fink, H. R. Freche, Equilibrium relations in aluminum–chromium alloys of high purity. Trans. Am. Soc. Met. AIME. 104, 325–334 (1933).

[1945, Raynor] G. V. Raynor, K. Little, The constitution of the aluminium-rich alloys of aluminium, chromium, and manganese. J. Inst. Met. 71, 493–524 (1945).

[1980, Eremenko] V. N. Eremenko, Y. V Natanzon, V. P. Titov, Kinetics of chromium dissolution in aluminum at 700-900 °C. Izv. Akad. Nauk SSSR. Metall. 6, 217–220 (1980).

[2017c, Chen] H.-L. Chen, "Thermodynamic modeling of the Al-Sn-X (X = Cd, Cu, In, Si, Zn) ternary systems" (Stockholm, Sweden, 2017), unpublished work.

Al-Ce-Mg

High-performance and lightweight aluminum-cerium alloys are recently reported to be potential candidates for high-temperature applications [2017, Sims]. Ce and many related systems have been added since TCS Al-based Alloy Database version 5 (TCAL5).

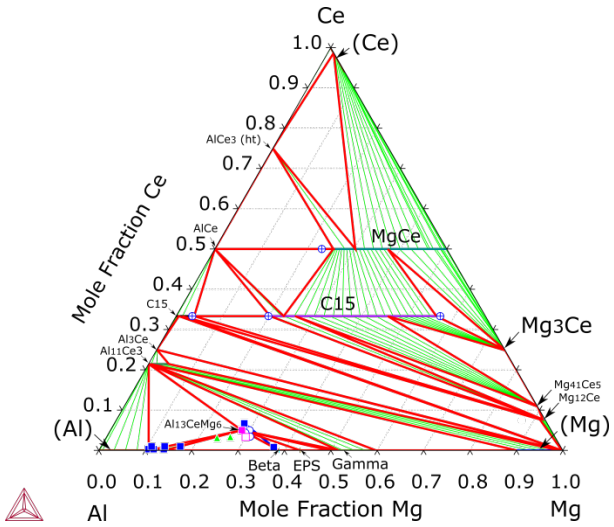

Figure 35: Al-Ce-Mg isothermal section at 400 °C [Chen, 2017].

References

[2017d, Chen] H.-L. Chen, "Thermodynamic modeling of the Al-Ce-X (X = Cr, Fe, Mg, Mn, Ni, Si) ternary systems" (Stockholm, Sweden, 2017), unpublished.

[2017, Sims] Z. C. Sims, O. R. Rios, D. Weiss, P. E. A. Turchi, A. Perron, J. R. I. Lee, T. T. Li, J. A. Hammons, M. Bagge-Hansen, T. M. Willey, K. An, Y. Chen, A. H. King, S. K. McCall, High performance aluminum–cerium alloys for high-temperature applications. Mater. Horizons. 4, 1070–1078 (2017).

Molar Volume and Related Examples

The TCS Al-based Alloy Database (TCAL) contains a database of molar volume and thermal expansion coefficients of all phases.

The TCS Al-based Alloy Database includes molar volume and thermal expansion coefficients of all phases starting with version 2 (TCAL2).

You can find information on our website about the thermophysical properties that can be calculated with Thermo-Calc and the Add-on Modules. Additional resources will also be made available on our website in the near future so keep checking back or subscribe to our newsletter.

The database can be used for:

- Calculating the molar volume (and thus the density) of the (Al) solid solution (Figure 36).
- Predicting the casting shrinkage of aluminum alloys (Figure 37).
- Calculating the thermal expansion (Figure 38)
- Predicting the lattice mismatch between a precipitate and the (Al) matrix phase (Figure 39)

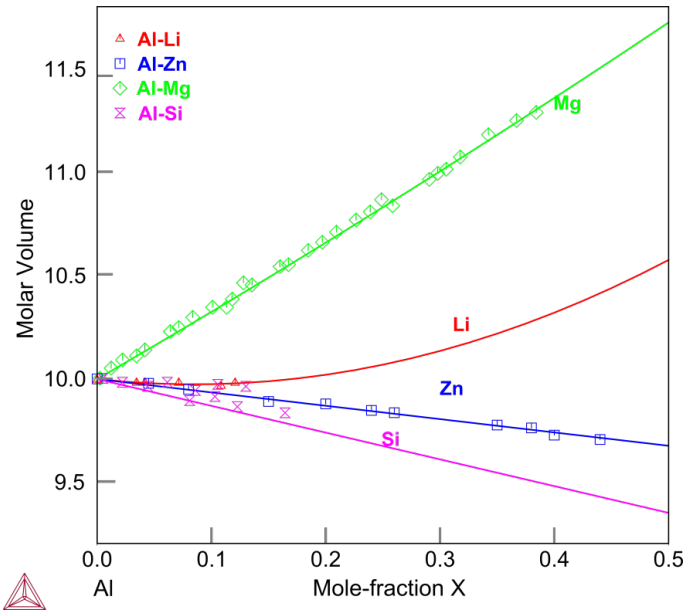

Figure 36: Calculated molar volumes of the Al-X (X=Li, Mg, Si, Zn) fcc_A1 phase.

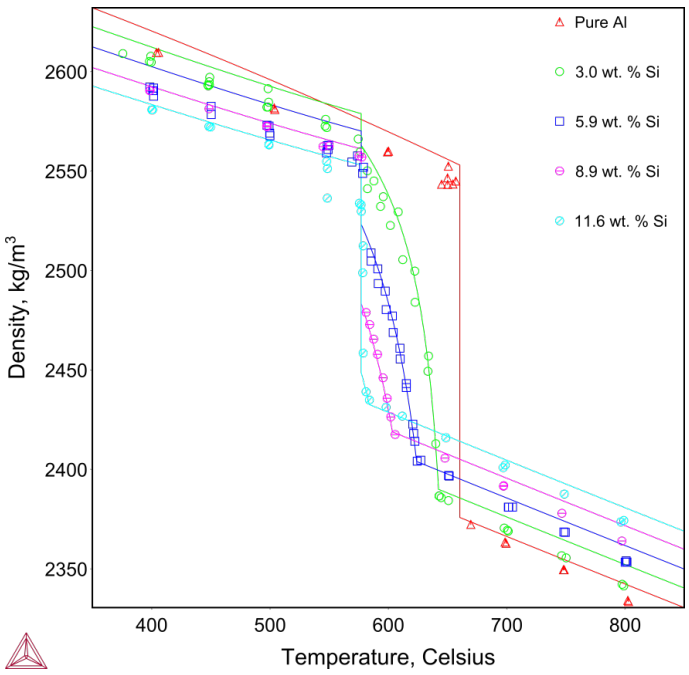

Figure 37: Calculated densities of pure Al and Al-Si alloys versus the temperature, in comparison with experimental data from Magnusson and Arnberg [2001].

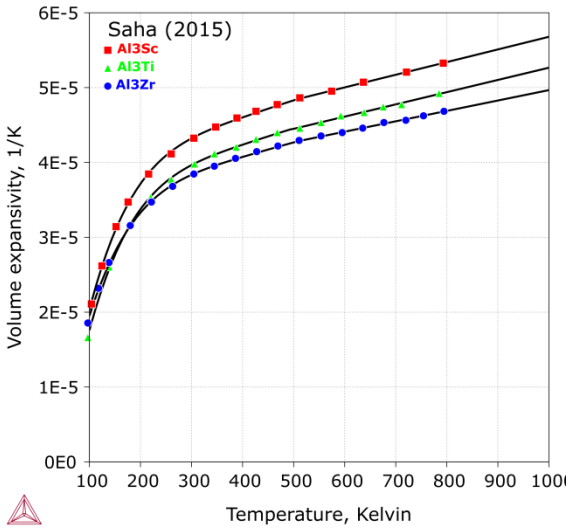

Figure 38: Calculated volume thermal expansivity for Al_3Sc, Al_3Ti and Al_3Zr [2017, Chen].

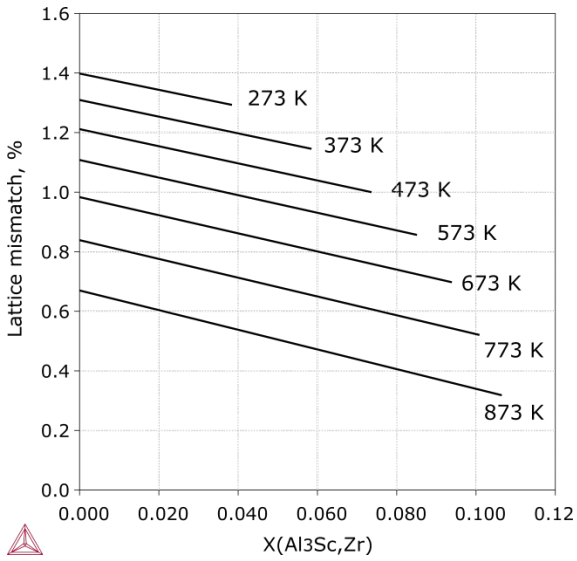

Figure 39: Lattice mismatch between Al_3Sc and (Al), at different Zr contents and temperatures [2017, Chen].

References

[2001, Magnusson] T. Magnusson, L. Arnberg, Density and solidification shrinkage of hypoeutectic aluminum-silicon alloys. Metall. Mater. Trans. A. 32, 2605–2613 (2001).

[2017e, Chen] H.-L. Chen, "Thermodynamic modeling of phase equilibria and molar volume in the Sc-Ti, Al-Sc-Si, Al-Sc-Ti, Al-Sc-Zr and Al-Si-Ti systems" (Stockholm, Sweden, 2017), unpublished work.

Metastable Phases / Precipitates

Most important precipitates that form during aging treatments and casting of aluminum alloys are metastable, except for a few such as Al_3Sc and Al_3Er (both modeled as AL3X). This example uses the TCS Al-based Alloy Database (TCAL).

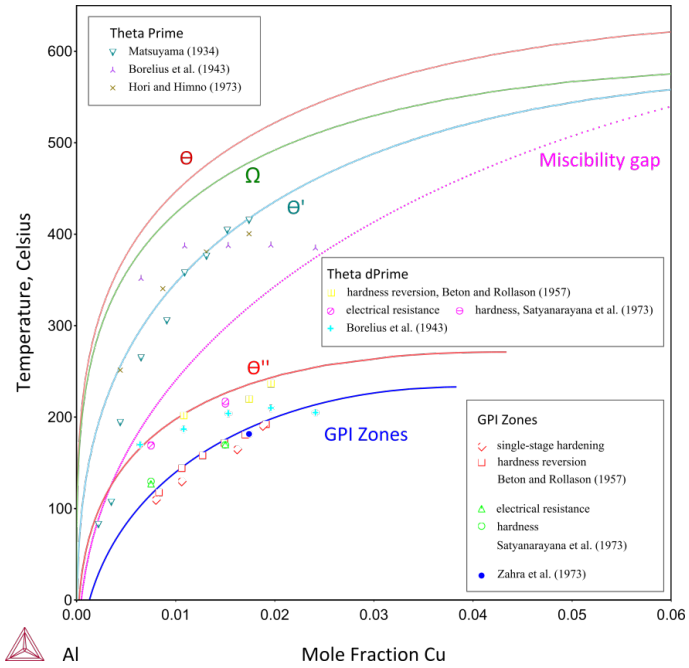

Figure 40: Calculated Al-Cu (Al) solvus curves equilibrated with θ, Ω, θ', θ'' (or GPII zones) and GPI zones, respectively. A metastable miscibility gap of fcc_A1 is shown. The GPI zones are modeled as the second composition set of fcc_A1, i.e. fcc_A1#2. It is assumed that experimentally observed GPI zones are usually tiny (say < 3 nm), so the interfacial and elastic energy are considered. The line for GPI zones is calculated with adding +800 J/mole-atoms to the energy of fcc_A1#2 [2014, Chen].

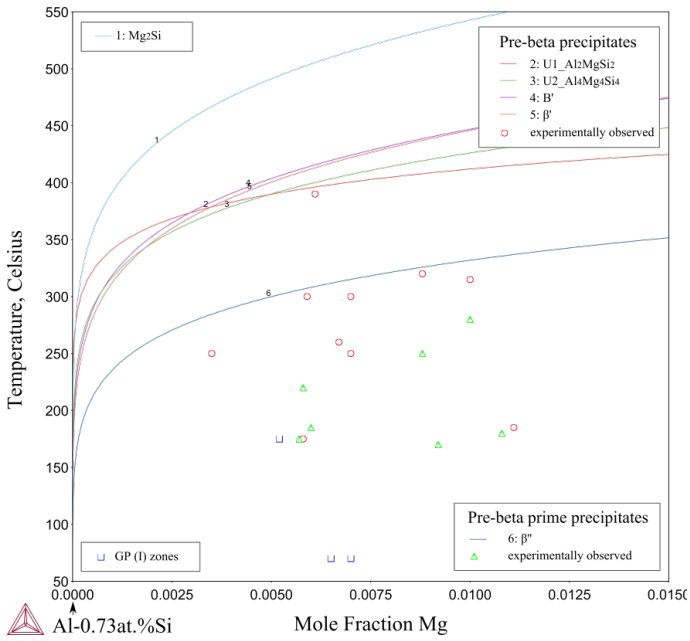

Figure 41: Calculated fcc_A1 solvi in alloys at 0.73 at.% Si and varying Mg content, relative to different Al-Mg-Si precipitates, including the stable β-Mg_2Si phase, pre-β precipitates (β', U1, U2 and B')and the pre-β' precipitate, i.e. β''. The symbols indicate certain precipitates have been experimentally observed in alloys of given compositions and aged at given temperatures [2014, Chen].

Reference

[2014b, Chen] H.-L. Chen, "Thermodynamic modeling of metastable precipitate phases in Al-Cu, Al-Fe, Al-Mg-Si, and Al-Mg-Zn based alloys" (Stockholm, Sweden, 2014), unpublished work.

Electrical Resistivity and Thermal Conductivity

Electrical resistivity and thermal conductivity of Al alloys are both of great importance since the alloys are widely used as electrical cables and radiators in cars and refrigerators. Moreover, thermal conductivity data are needed for designing processes in additive manufacturing.

Using Thermo-Calc with the TCS Al-based Alloy Database (TCAL), you can calculate the quantities of a phase ϕ, with the variables ELRS(ϕ) and THCD(ϕ) or a system (i.e. alloy), with ELRS and THCD. You can also calculate derived quantities, including electrical conductivity (ELCD), thermal resistivity (THRS) and thermal diffusivity (THDF) in a similar way.

The TCS Al-based Alloy Database includes electrical resistivity (*ELRS*) and thermal conductivity (*THCD*) starting with version 7 (TCAL7).

You can find information on our website about the thermophysical properties that can be calculated with Thermo-Calc and the Add-on Modules. Additional resources will also be made available on our website in the near future so keep checking back or subscribe to our newsletter.

Al Electrical Resistivity

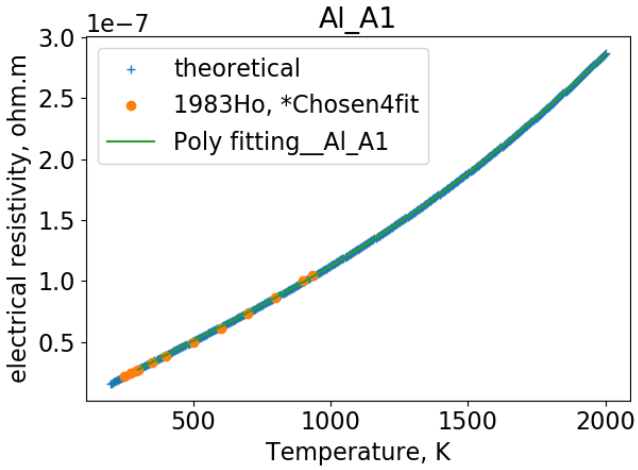

Figure 42: The modeling of electrical resistivity (ELRS) of FCC_A1 Al. Theoretical model and parameters is first fitted to the data from Ho [1983] and extrapolated to high temperatures, say 2000 K. A polynomial is then fitted to the data and the extrapolated values and the resulting parameters are stored in the database. Such treatments benefit from the simplicity using polynomials and guarantee the reliability for the extrapolation.

Ni Electrical Resistivity

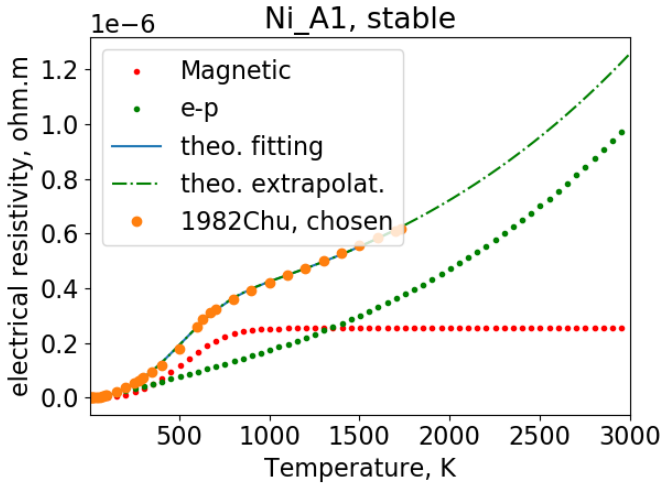

Figure 43: The modeling of electrical resistivity (ELRS) of FCC_A1 Ni. The description has contributions from intrinsic resistivity due to electron-phone processes (the green dotted line) and magnetic resistivity due to spin disordering (the red dotted line), as well as residual resistivity, which is insignificant. Note that you will only get the total resistivity (the light green dotted-dashed line) with Thermo-Calc. The golden symbols are experimental data from Chu [1982].

Cu Thermal Resistivity

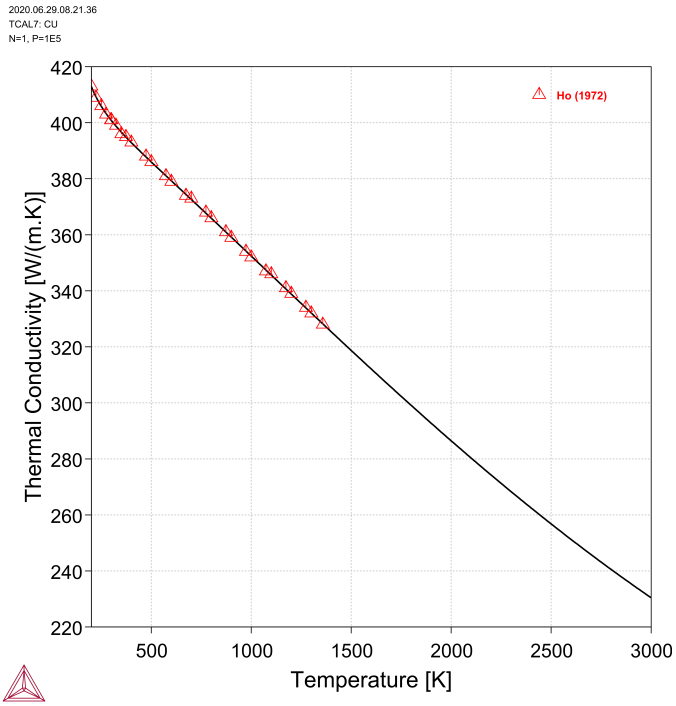

Figure 44: Calculated thermal resistivity (THCD) of FCC_A1 Cu, which is an important alloying element to several series of aluminum alloys. The data are from Ho [1972]. Note that the extrapolation might not be valid beyond 3000 K.

Al-Mg Electrical Resistivity

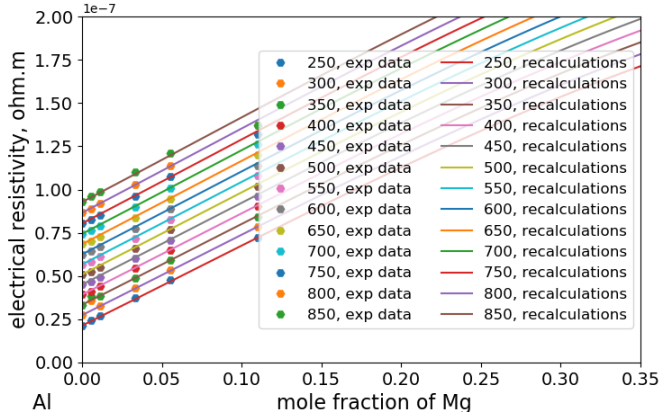

Figure 45: The modeling of electrical resistivity (ELRS) of the FCC_A1 phase in the Al-Mg binary, which is a core system to aluminum alloys. Experimental data are from Ho [1983]. Based on the Al-Mg phase diagram, it is suspected that certain alloys might contain ALMG_BETA depending on the metallurgy history and the alloy composition.

References

[1972, Ho] C. Y. Ho, R. W. Powell, P. E. Liley, Thermal Conductivity of the Elements, J.Phys. Chem. Reference Data 1, 279-421 (1972).

[1982, Chu] T. K. Chu, C. Y. Ho, Electrical resistivity of Chromium, Cobalt, Iron, and Nickel, CINDAS Report 60, June 1982.

[1983, Ho] C. Y. Ho, M. W. Ackerman, K. Y. Wu, T. N. Havill, R. H. Bogaard, R. A. Matula, S. G. Oh, H. M. James, Electrical Resistivity of Ten Selected Binary Alloy Systems, J. Phys. Chem. Reference Data 12, 183-322 (1983).

TCAL References

This section is a collation of references related to the database diagrams and plots. There are additional references specific to the database itself that can be listed when using the database within Thermo-Calc.

[1933, Fink] W. L. Fink, H. R. Freche, Equilibrium relations in aluminum–chromium alloys of high purity. Trans. Am. Soc. Met. AIME. 104, 325–334 (1933).

[1940, Takeda] S. Takeda, K. Mutuzaki, The equilibrium diagram of the Fe–Al–Si system. Tetsu-to-Hagane. 26, 335–361 (1940).

[1945, Raynor] G. V. Raynor, K. Little, The constitution of the aluminium-rich alloys of aluminium, chromium, and manganese. J. Inst. Met. 71, 493–524 (1945).

[1948, Strawbridge] D. J. Strawbridge, A. Little, The Constitution of Aluminium Copper Magnesium Zinc Alloys At 460 °C. J. Inst. Met. 74, 191–225 (1948).

[1956, Wright] E. H. Wright, “Equilibrium relations at 460 °C in aluminum-copper-magnesium-zinc alloys of high purity” (Internal Report 13–56-EC2, Aluminum Research Laboratories, Aluminum Company of America, 1956).

[1967, Munson] D. Munson, A Clarification of the Phases Occurring in Aluminium-Rich Aluminium-Iron-Silicon Alloys, with Particular Reference to the Ternary Phase α-AlFeSi. J. Inst. Met. 95, 217–219 (1967).

[1972, Ho] C. Y. Ho, R. W. Powell, P. E. Liley, Thermal Conductivity of the Elements, J.Phys. Chem. Reference Data 1, 279-421 (1972).

[1980, Eremenko] V. N. Eremenko, Y. V Natanzon, V. P. Titov, Kinetics of chromium dissolution in aluminum at 700-900 °C. Izv. Akad. Nauk SSSR. Metall. 6, 217–220 (1980).

[1982, Chu] T. K. Chu, C. Y. Ho, Electrical resistivity of Chromium, Cobalt, Iron, and Nickel, CINDAS Report 60, June 1982.

[1983, Ho] C. Y. Ho, M. W. Ackerman, K. Y. Wu, T. N. Havill, R. H. Bogaard, R. A. Matula, S. G. Oh, H. M. James, Electrical Resistivity of Ten Selected Binary Alloy Systems, J. Phys. Chem. Reference Data 12, 183-322 (1983).

[1986, Fujikawa] S. Fujikawa, Solvuses of delta’ phase (Al3Li) and delta phase (AlLi) in Al-Li alloys. J. Japan Inst. Light Met. 36, 771–777 (1986).

[1988, Zakharov] A. M. Zakharov, I. T. Gulman, A. A. Arnold, Y. A. Matsenko, Phase diagram of the Aluminium-Silicon-Iron system in the concentration range of 10-14% Si and 0-3% Fe. Russ. Metall. 3, 177–180 (1988).

[1989, Saunders] N. Saunders, Calculated stable and metastable phase equilibria in Al-Li-Zr alloys. Zeitschrift fur Met. 80, 894–903 (1989).

[1990, Backerud] L. Backerud, G. Chai, J. Tamminen, Solidification Characteristics of Aluminum Alloys in Foundry Alloys, Volume 1 and 2 (American Foundrymen's Society, Inc., 1990), p. 266.

[1992, Tundal] U.H. Tundal, N. Ryum, Dissolution of particles in binary alloys: part II. experimental investigation on an Al-Si alloy, Metall. Trans. A 23 (1992) 445–449.

[2001, Magnusson] T. Magnusson, L. Arnberg, Density and solidification shrinkage of hypoeutectic aluminum-silicon alloys. Metall. Mater. Trans. A. 32, 2605–2613 (2001).

[2002, NDT] Conductivity and Resistivity Values for Aluminum & Alloys, Compiled by the Collaboration for NDT Education, March 2002.

[2004, Bosselet] F. Bosselet, S. Pontevichi, M. Sacerdote-Peronnet, J. C. Viala, Experimental measurement of the Al-Fe-Si isothermal section at 1000 K. J. Phys. IV. 122, 41–46 (2004).

[2004, Pontevichi] S. Pontevichi, F. Bosselet, F. Barbeau, M. Peronnet, J. C. Viala, Solid-liquid phase equilibria in the Al-Fe-Si system at 727 °C. J. Phase Equilibria Diffus. 25, 528–537 (2004).

[2005, Kurum] E. C. Kurum, H. B. Dong, J. D. Hunt, Microsegregation in Al-Cu Alloys. Metall. Mater. Trans. A, 36, 3103 (2005).

[2010, Marlaud] T. Marlaud, A. Deschamps, F. Bley, W. Lefebvre, B. Baroux, "Influence of alloy composition and heat treatment on precipitate composition in Al-Zn-Mg-Cu alloys", Acta Mater. 58 (2010) 248-260.

[2012a, Chen] H.-L. Chen, "Modeling of the AlLi2 and Al3Li phases in the Al-Li binary system", unpublished work, 2012a/2017b.

[2012, Liu] K. Liu, X. Cao, X. G. Chen, A New Iron-Rich Intermetallic-Al m Fe Phase in Al-4.6Cu-0.5Fe Cast Alloy. Metall. Mater. Trans. A. 43, 1097–1101 (2012).

[2012b, Chen] H.-L. Chen, "Thermodynamic assessment of the Al-Cu-Mg-Zn(-Fe) and Al-Cu-Mg-Si multicomponent alloy systems" (Stockholm, Sweden, 2012), unpublished work.

[2014a, Chen] H. Chen, Q. Chen, Y. Du, J. Bratberg, A. Engström, Update of Al-Fe-Si, Al-Mn-Si and Al-Fe-Mn-Si thermodynamic descriptions - TNMSC. Chinese J. Nonferrous Met. 24, 2041–2053 (2014).

[2014b, Chen] H.-L. Chen, "Thermodynamic modeling of metastable precipitate phases in Al-Cu, Al-Fe, Al-Mg-Si, and Al-Mg-Zn based alloys" (Stockholm, Sweden, 2014), unpublished work.

[2016, Jin] K. Jin, B. C. Sales, G. M. Stocks, G. D. Samolyuk, M. Daenen, W. J. Weber, Y. Zhang, H. Bei, Tailoring the physical properties of Ni-based single-phase equiatomic alloys by modifying the chemical complexity, Scientific Reports 6, 20159 (2016).

[2017a, Chen] H.-L. Chen, "Thermodynamic modeling of the Er-X (X = Ag, Al, Fe, Si, Zr) binary and Al-Er-X (X=Cu, Fe, Mg) ternary systems" (Stockholm, Sweden, 2017), unpublished work.

[2017b, Chen] H.-L. Chen, "Modeling of the AlLi2 and Al3Li phases in the Al-Li binary system", unpublished work, 2012a/2017b.

[2017c, Chen] H.-L. Chen, "Thermodynamic modeling of the Al-Sn-X (X = Cd, Cu, In, Si, Zn) ternary systems" (Stockholm, Sweden, 2017), unpublished work.

[2017d, Chen] H.-L. Chen, "Thermodynamic modeling of the Al-Ce-X (X = Cr, Fe, Mg, Mn, Ni, Si) ternary systems" (Stockholm, Sweden, 2017), unpublished work.

[2017e, Chen] H.-L. Chen, "Thermodynamic modeling of phase equilibria and molar volume in the Sc-Ti, Al-Sc-Si, Al-Sc-Ti, Al-Sc-Zr and Al-Si-Ti systems" (Stockholm, Sweden, 2017), unpublished work.

[2017, Sims] Z. C. Sims, O. R. Rios, D. Weiss, P. E. A. Turchi, A. Perron, J. R. I. Lee, T. T. Li, J. A. Hammons, M. Bagge-Hansen, T. M. Willey, K. An, Y. Chen, A. H. King, S. K. McCall, High performance aluminum–cerium alloys for high-temperature applications. Mater. Horizons. 4, 1070–1078 (2017).

[2019, Razaz] G. Razaz, T. Carlberg, Hot Tearing Susceptibility of AA3000 Aluminum Alloy Containing Cu, Ti, and Zr, Metall. Mater. Trans. A Phys. Metall. Mater. Sci., (2019).